



# Oxy-steam reforming of methanol on copper catalysts

Pawel Mierczynski<sup>1</sup> · Magdalena Mosinska<sup>1</sup> · Waldemar Maniukiewicz<sup>1</sup> ·  
Magdalena Nowosielska<sup>1</sup> · Agnieszka Czylkowska<sup>1</sup> · Malgorzata I. Szykowska<sup>1</sup>

Received: 1 April 2019 / Accepted: 27 May 2019 / Published online: 14 June 2019  
© The Author(s) 2019

## Abstract

The influence of copper content in the monometallic catalysts supported on the  $\text{CeO}_2\text{-Al}_2\text{O}_3$  binary oxide system on their catalytic activity and physicochemical properties in oxy-steam reforming of methanol was investigated. It was shown that activity and selectivity depends on the content of copper, its dispersion on the catalysts surface. It was confirmed that optimal copper content was 20 wt% of Cu. Copper catalysts with 20 wt% of Cu exhibited the highest methanol conversion and reaction rate value compared to the rest of the investigated catalysts systems. The kinetic measurements performed in oxy-steam reforming of methanol on 20%Cu/ $\text{CeO}_2\text{-Al}_2\text{O}_3$  catalysts, showed an activation energy for this system equal  $E_a(\text{OSRM}) = 66.56 \text{ kJ/mol}$ .

**Keywords** Reforming of methanol · Hydrogen production · Copper catalysts · Binary oxide ·  $\text{CeO}_2\text{-Al}_2\text{O}_3$  · Reforming of methanol · OSRM

## Introduction

Currently, the depletion of natural fossil fuel resources and rising prices cause that humanity around the world are focused their research interest in development of others source of energy. One of the possible solutions of this problem is fuel cell technology powered by hydrogen easily accessible on earth [1]. The use of hydrogen as an energy raw material is a hot topic for several years. The development of energy technologies using hydrogen leads to the fact that it has become one of the most environmentally friendly fuels. The advantage of using hydrogen as a fuel is primarily its pro-ecological nature. The combustion process of hydrogen generates only water vapour and nitrogen oxides (in much lower quantities compared to the combustion of fossil fuels). However, when the hydrogen oxidation process is carried out

---

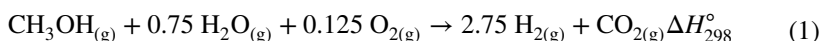
✉ Pawel Mierczynski  
pawel.mierczynski@p.lodz.pl; mierzczyn25@wp.pl

<sup>1</sup> Institute of General and Ecological Chemistry, Lodz University of Technology, Zeromskiego 116, 90-924 Lodz, Poland

in fuel cells, the only by-product is water vapour. Hydrogen itself can be produced potentially from liquid hydrocarbons such as methanol [2, 3], ethanol [4], dimethyl ether [5] and others. However, the most preferred is methanol, which offers many advantages in the hydrogen production because of the following reasons [6, 7]:

- Methanol is the simplest alcohol with a high carbon to hydrogen ratio (1:4);
- Lack of C–C bond in the methanol molecule;
- It is easily reformed;
- It can be obtained from biomass.

All of these properties make that methanol can become an energy carrier in the future [8]. Hydrogen can produced via steam reforming of methanol, partial oxidation of methanol or using the combination of these two processes in one act of reaction named oxy-steam reforming of methanol (OSRM) according to the following equation (Eq. 1):



The oxy-steam reforming of methanol reaction can be carried out in the auto-thermal way. That is why from the application point of view oxy-steam reforming process is energetically favourable because it does not require any external heat when it is run. Typical catalysts used in oxy-steam reforming process are monometallic copper [9] or nickel [10] and bimetallic M-Cu copper supported catalysts (where M = Ru, Rh, Pd, Ir) [11–13]. Cerium oxide are widely used as an additive to the catalyst support and an essential component of the automotive three-way converter (TWC) [14]. It is also well known as a modifier affecting on the catalyst reactivity. CeO<sub>2</sub> improves the degree of metal dispersion of the active phase and the redox behaviour of the supported catalysts systems. Cerium oxide based catalysts are also characterized by the strong metal-carrier interactions and high oxygen transfer capacity [15–17]. In addition, copper supported catalysts owned high catalytic activity and selectivity to the main products in reforming of methanol processes. Chang et al. [18]. reported that cerium oxide increased the reducibility of the catalyst, but not influence on reactivity results in OSRM process. It was also found that CeO<sub>2</sub> did not suppress CO formation in the presence of O<sub>2</sub>. It is well known from the literature review that copper based catalysts are used in reforming of methanol processes [19–22], CO oxidation [23–25], water gas shift reaction (WGS) [26–30], methanol synthesis [31–33] and hydrogenation of furfural process [34, 35]. All these suggestions confirm that it is worth determining the catalytic and physicochemical properties of copper catalysts supported on alumina-ceria binary oxide in the methanol reforming process.

Based on our previous studies, we decided to prepare monometallic copper catalysts instead of well-known bimetallic systems due to the fact that monometallic copper catalysts are much cheaper and are in some cases characterized by higher activity and selectivity in the investigated process [11]. In addition, we chose binary oxide as a carrier of our catalytic systems composed of aluminum and cerium oxides with the following composition CeO<sub>2</sub>·Al<sub>2</sub>O<sub>3</sub>. We selected the Ce:Al ratio equal 1:2 in the carrier because of the fact that binary systems containing higher content of

$\text{Al}_2\text{O}_3$  exhibited higher specific surface area and activity in the studied oxy-steam reforming of methanol process compared to the catalyst with low content of  $\text{Al}_2\text{O}_3$ . In the present work, we decided to prepare monometallic copper catalysts supported on binary oxide  $\text{CeO}_2\cdot\text{Al}_2\text{O}_3$  containing various content of Cu by conventional wet impregnation method. Prepared catalytic materials were extensively studied by various techniques such as: TPR- $\text{H}_2$ , TPD- $\text{NH}_3$ , XRD, SEM-EDS, BET, CO chemisorption techniques. We also described the correlation between the physicochemical and catalytic properties of copper catalysts in oxy-steam reforming of methanol process. In addition, the kinetics studies performed in oxy-steam reforming of methanol process were presented in the manuscript.

## Experimental

### Preparation of the catalytic material

#### Supports

Binary oxide  $\text{CeO}_2\cdot\text{Al}_2\text{O}_3$  system were prepared by co-precipitation method. In order to prepare binary oxides the following molar ratio of Ce:Al = 1:2 were used. Aqueous solutions of 1 mol/L cerium nitrate and 1 mol/L aluminium nitrate were mixed in appreciate quantity under vigorous stirring at 80 °C. A concentrated ammonia solution was then added by dropwise addition until the pH reached values between 10 and 11. Then the mixture was stirred for another 30 min. The resulting fine precipitate was then washed two times in deionised water and then dried at 120 °C for 15 h and calcined for 4 h at 400 °C in air atmosphere.

#### Catalysts preparation

Copper supported catalysts  $\text{Cu}/\text{CeO}_2\cdot\text{Al}_2\text{O}_3$  were prepared by wet aqueous impregnation method. Metal phase Cu was introduced on the binary oxide by wet impregnation method using aqueous solutions of copper nitrate (V). Impregnation lasted 12 h. Copper loading on the catalyst surface was 5, 20, 40 and 60 wt%. The obtained supported catalysts were then dried for 2 h at 120 °C and calcined for 4 h in an air atmosphere at 400 °C.

### Characterisation methods

#### Specific surface area (BET method)

The specific surface area and porosity of supports and catalysts were determined by the BET based on low temperature (−196 °C) nitrogen adsorption in a Micromeritics ASAP 2020 apparatus.

### Temperature programmed reduction (TPR-H<sub>2</sub>)

The TPR-H<sub>2</sub> measurements were carried out in an automatic TPR system AMI-1 in the temperature range of 25–900 °C with a linear heating rate of 10 °C min<sup>-1</sup>. Samples (weight about 0.1 g) were reduced in hydrogen stream (5% H<sub>2</sub>–95% Ar) with a volumetric flow rate of 40 cm<sup>3</sup> min<sup>-1</sup>. Hydrogen consumption was monitored during the measurements by a thermal conductivity detector (TCD detector).

### Temperature programmed desorption (TPD-NH<sub>3</sub>)

The TPD-NH<sub>3</sub> measurements were carried out in a quartz microreactor using NH<sub>3</sub> as a probe molecule. The NH<sub>3</sub> was adsorbed on the samples surface at 50 °C for 30 min after the purification process of the catalyst surface performed in a flowing He stream at 600 °C for 60 min. The temperature programmed desorption of NH<sub>3</sub> was carried out in the temperature range 100–600 °C using a linear growth of temperature (25 °C min<sup>-1</sup>) using a thermal-conductivity detector. Before each experiment physically adsorbed ammonia has been removed from the catalytic material surface.

### X-ray diffraction (XRD) measurements

Room temperature powder X-ray diffraction patterns were collected using a PANalytical X'Pert Pro MPD diffractometer in Bragg–Brentano reflecting geometry. Copper Cu K<sub>α</sub> radiation from a sealed tube was used. Data was collected in the range 5–90° 2 $\theta$  with a step of 0.0167° and exposure per step of 27 s. Due to the fact that raw diffraction data contain some noise, the background during the analysis was subtracted using Sonneveld and Visser algorithm. The data was then smoothed using cubic polynomial.

All calculations were done using X'PertHighScore Plus computer software.

### CO chemisorption measurements

Carbon monoxide chemisorption analyses were carried out in a Micromeritics ASAP 2020 apparatus. Prior to CO chemisorptions, all catalysts were reduced in situ at 300 °C in the 5% H<sub>2</sub>–95% Ar mixture for 2 h. After the reduction, the samples were cooled to 35 °C under helium stream. The chemisorbed carbon monoxide was analyzed at 35 °C using the adsorption–back sorption isotherm method.

### Catalytic activity tests

The oxy-steam reforming of methanol (OSRM) was performed using a flow microreactor under atmospheric pressure. The reaction was carried out in the temperature range 90–200 °C. HPLC grade methanol (Aldrich, water ~0.03 wt%) was used in each catalytic test. The catalyst load was 0.2 g and the stream composition was: H<sub>2</sub>O/CH<sub>3</sub>OH/O<sub>2</sub> = 1/1/0.4 (molar ratio) and the GHSV was 26,700 h<sup>-1</sup> (calculated at

ambient temperature and under atmospheric pressure). The total flow rate was kept at 31.5 ml/min. Argon was used as the balance gas. The steady-state activity measurements at each temperature were taken after at least 2 h on stream. The analysis of the organic products (methanol, methane, methyl formate, dimethyl ether (DME), formaldehyde) was carried out by an on-line gas chromatograph equipped with a FID detector and 10% Carbowax 1500 on Graphpac column. The CO, CH<sub>4</sub> and CO<sub>2</sub> concentrations were followed by a gas chromatograph equipped with a TCD detector (150 °C, 60 mA), and Carbopshere 60/80 (50 °C) column. The hydrogen concentration was measured by GC equipped with TCD detector (120 °C, 60 mA) and molecular sieve 5a (120 °C) column. Material balances on carbon were calculated to verify the obtained results. The selectivity towards the formation of hydrogen, carbon monoxide, carbon dioxide and DME in OSRM were calculated using Eqs. 1–4 and the conversion of methanol using Eq. 5:

$$S_{H_2}(\%) = \frac{(nH_{2-out})}{\sum \text{product of the reaction}} \times 100 \quad (2)$$

$$S_{CO}(\%) = \frac{(nCO_{out})}{\sum \text{products of the reaction}} \times 100 \quad (3)$$

$$S_{CO_2}(\%) = \frac{(nCO_{2-out})}{\sum \text{product of the reaction}} \times 100 \quad (4)$$

$$S_{CO_2}(\%) = \frac{(nDME_{out})}{\sum \text{product of the reaction}} \times 100 \quad (5)$$

Here,  $n_{CH_3OH}$  and  $n_{H_2}$  is the molar flow rate of CH<sub>3</sub>OH and H<sub>2</sub>, respectively.

$$\text{Conv.}_{CH_3OH} = \frac{n_1^{\text{in}} CH_3OH - n_2^{\text{out}} CH_3OH}{n_1^{\text{in}} CH_3OH} \times 100 \quad (6)$$

here  $nH_{2-out}$ —mole of H<sub>2</sub> in the feed out,  $nCO_{2-out}$ —mole of CO<sub>2</sub> in the feed out,  $nCO_{out}$ —mole of CO in the feed out,  $nDME_{out}$ —mole of DME in the feed out,  $n_1^{\text{in}}CH_3OH$ ,  $n_1^{\text{in}}CH_3OH$ ,  $n_2^{\text{in}}CH_3OH$ ,  $n_2^{\text{out}}CH_3OH$ —mole of CH<sub>3</sub>OH in the feed in and in the feed out, Methane, formaldehyde and methyl formate formation were not observed during the reaction. Only carbon monoxide and dimethyl ether were formed during the reaction as intermediates.

The kinetic studies were performed for the selected catalysts using micro-fixed bed reactor operating at low conversions of methanol in order to limit the diffusion process and changes of the reactants during an investigated experiment. The kinetics measurements were done below 10% of the methanol conversion value. The reaction products contain only H<sub>2</sub>, CO<sub>2</sub>, and CO compounds in the eluent gas independently on the reaction temperature. These results confirm that only steam and partial oxidation of methanol processes took place in the investigated temperatures. Activation

energy in OSRM process was determined for the selected catalysts. The reaction rate in OSRM process was calculated based on the equation presented below

$$-dF = F^0 dX_{CH_3OH} = (-r_{CH_3OH})dW$$

Here  $F^0$ —flow rate of methanol,  $X_{CH_3OH}$ —is the methanol conversion,  $W$ —catalyst weight,  $r_{CH_3OH}$ —reaction rate of methanol. The appropriate transformation of the above presented equation gives the assumption, that the reaction rate is equal:  $(-r_{CH_3OH}) = \frac{dX_{CH_3OH}}{d\left(\frac{W}{F^0}\right)}$ .

## Results and discussion

The values of specific surface area, monolayer capacity and average pore radius for  $CeO_2 \cdot Al_2O_3$  and various  $Cu/CeO_2 \cdot Al_2O_3$  (metal loading = 5, 20, 40 and 60 wt%) catalysts are presented in Table 1. The obtained results showed that the investigated catalysts had specific surface area in the range of 30–170  $m^2/g$ . The highest value of SSA and monolayer capacity owned binary oxide support ( $CeO_2 \cdot Al_2O_3$ ). Introduction of copper oxide onto the support surface result in decrease of the specific surface area. The specific surface area decreases parallel with increase of copper content in the investigated catalysts. This phenomenon is explained by blocking of the support pore by the metal oxide created during the preparation step of the catalyst. The value of the monolayer capacity for 5%  $Cu/CeO_2 \cdot Al_2O_3$ , 20%  $Cu/CeO_2 \cdot Al_2O_3$  and 40%  $Cu/CeO_2 \cdot Al_2O_3$  are in the range 20.7–28.9  $cm^3/g$ .

In the meantime, in the case of the 60%  $Cu/CeO_2 \cdot Al_2O_3$  catalyst, the value of monolayer capacity was significantly lower compared to the rest of the copper supported catalysts. The pore size distribution of support ( $CeO_2 \cdot Al_2O_3$ ) and monometallic copper supported  $Cu/CeO_2 \cdot Al_2O_3$  (metal loading = 5, 20, 40 and 60 wt%) catalysts is presented in Fig. 1. The average pore size results showed that binary oxide support ( $CeO_2 \cdot Al_2O_3$ ) and 20%  $Cu/CeO_2 \cdot Al_2O_3$  catalyst have an average pore size of about 2.1 nm. Whereas, the monometallic copper supported catalysts systems containing 5 wt% and 40 wt% of copper have an average pore size equal to 7 and 8 nm, respectively.

It is worth mentioning that these catalytic systems are characterized by inhomogeneous pore size. On the other hand, in the case of 60%  $Cu/CeO_2 \cdot Al_2O_3$  catalyst,

**Table 1** BET surface area, monolayer capacity and average pore radius results for various  $Cu/CeO_2 \cdot Al_2O_3$  (metal loading = 5, 20, 40 and 60 wt%) catalysts calcined in air atmosphere at 400 °C for 4 h

Material	BET surface area ( $m^2/g$ )	Monolayer capacity ( $cm^3/g$ )	Average pore radius (nm)
$CeO_2 \cdot Al_2O_3$	170	40	2.1
5% $Cu/CeO_2 \cdot Al_2O_3$	126	28.9	7
20% $Cu/CeO_2 \cdot Al_2O_3$	101	23.3	2.1
40% $Cu/CeO_2 \cdot Al_2O_3$	90	20.7	8
60% $Cu/CeO_2 \cdot Al_2O_3$	30	7.0	–

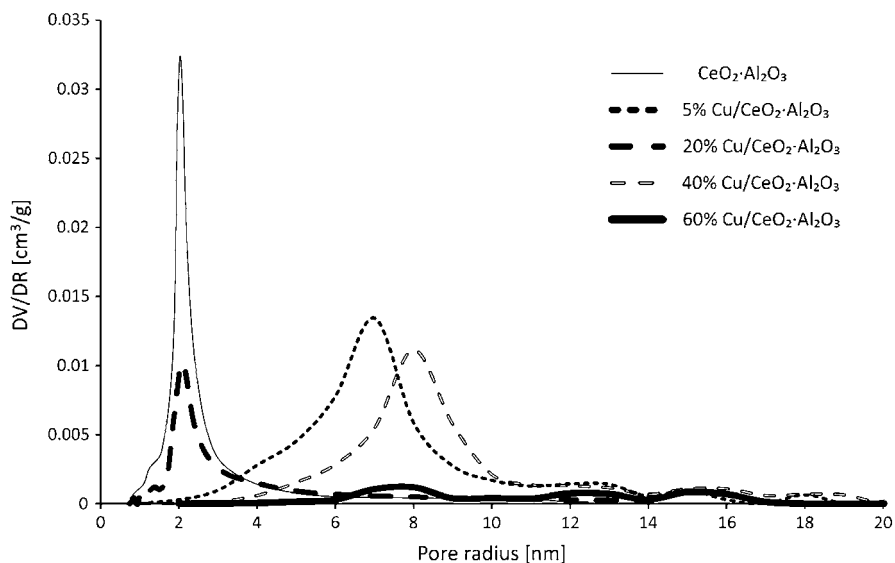


**Fig. 1** Pore radius distributions for monometallic Cu/CeO<sub>2</sub>·Al<sub>2</sub>O<sub>3</sub> (metal loading = 5, 20, 40 and 60 wt%) catalysts calcined at 400 °C in air atmosphere for 4 h

we can observe a three types of pore sizes distribution. This means that in the case of this system the average pore size cannot be directly determine. Chemisorption measurements and the results of the kinetic studies were given in Table 2. The results of dispersion degree of metallic copper and crystallites size for copper catalysts are given in the same table. As mentioned before, the introduction of copper ions onto the binary oxide CeO<sub>2</sub>·Al<sub>2</sub>O<sub>3</sub> results in decrease the value of specific surface area for investigated catalysts (see Table 1). The decrease of the specific surface area (BET) can be explained by the presence of larger crystallites of the copper oxide formed during preparation step, which are reduced during activation process to metallic copper. These results were confirmed by the metallic copper dispersion degree obtained on catalysts surface of the investigated catalysts. The results clearly showed that the catalyst containing 40 wt% of Cu exhibited the highest crystallite size equal about 818 nm. The highest copper dispersion degree exhibited (2.14%) 5%Cu/CeO<sub>2</sub>·Al<sub>2</sub>O<sub>3</sub> catalyst (see Table 2).

The catalytic properties of the investigated catalysts in OSRM were also investigated in this work. For the purpose of comparative activity of the tested catalysts, we determined the reaction rate and activation energy in the conversion range below 10%. Recently, much attention has been devoted to the determination of important catalyst performance metrics include the activity, selectivity and deactivation of the catalyst. All these values make it possible to compare the catalysts tested in the same reaction [36]. In the literature, data concerning the catalytic studies, various expression of the catalyst yield can be found which are widely used to compare the catalysts reactivity. The most commonly used are reaction rate, reaction rate constant, turnover frequency (TOF) and turnover

**Table 2** Reaction rates, activation energy, dispersion degree, CO sorption and crystallite size of Cu/CeO<sub>2</sub>/Al<sub>2</sub>O<sub>3</sub> (metal loading = 5, 20 and 40 wt%) catalysts calcined in an air atmosphere at 400 °C for 4 h

Catalyst	Metal dispersion (%)	S <sub>cat</sub> (m <sup>2</sup> /g <sub>cat</sub> )	Metal area (m <sup>2</sup> /g <sub>Me</sub> )	Crystallite size (nm)	<sup>a</sup> CH <sub>3</sub> OH conv. (%) at 100 °C	r (mol s <sup>-1</sup> g <sub>cat</sub> <sup>-1</sup> )	E <sub>a</sub> (kJ/mol)
5%Cu/CeO <sub>2</sub> /Al <sub>2</sub> O <sub>3</sub>	2.14	0.69	13.8	48.5	5.9	3.79 × 10 <sup>-7</sup>	69.63
20%Cu/CeO <sub>2</sub> /Al <sub>2</sub> O <sub>3</sub>	0.16	0.20	1.00	669	6.6	4.24 × 10 <sup>-7</sup>	66.56
40%Cu/CeO <sub>2</sub> /Al <sub>2</sub> O <sub>3</sub>	0.13	0.33	0.82	818	4.4	2.81 × 10 <sup>-7</sup>	73.21

Activation of catalysts: drying in air at 120 °C for 2 h, calcination in an air temperature at 400 °C for 4 h, reduction before activity tests in 5% H<sub>2</sub> - 95% Ar mixture at 300 °C, 2 h. Reaction conditions: T = 100 °C, m<sub>cat</sub> = 0.2 g, H<sub>2</sub>O/CH<sub>3</sub>OH/O<sub>2</sub> = 1/1/0.4 (molar ratio) and the GHSV was 26,700 h<sup>-1</sup>, feed flow rate = 31.5 mL/min

<sup>a</sup>Methanol conversion at T = 100 °C



number (TON) values are often used in catalysis research in order to express the catalytic performance [37, 38]. In particular the values of TOF and TON, are calculated based on simplifications that have a huge impact on the received their values. For example of the TOF and TON numbers are even used interchangeably [37]. However, from the point of view of expressing catalytic efficiency, they should have different meanings [38]. In the extreme case, the TOF value is even considered as a rate-constant, because of the fact that the rate of reaction ( $r = \text{TOF} \times [\text{Cat}]$ ) depends on the catalyst concentration [37]. The TOF number depends on the concentration of the reactants or the products formed in the process, thus being closer to the reaction rate and not to the constant rate, as reported by Kozuch and Martin [37]. Actually, TOFs number is a widely used term related to the catalytic center in relation to the term “rate of reaction”, which is closely related to the product formation or consumption of substrate.

Lente [38] reported that TOFs value should be considered as an additional tool using for characterizing activity of the catalysts although they do not fit to the concept of chemical kinetics [38]. He reported that it is not possible to reliably present the rate law with one physical property (e.g. TOF or TON number). In addition, he emphasized that the use of TOF does not take into account the stoichiometric coefficients contained in the chemical equation and also does not include non-catalyzed route. The author notes that in order to express the efficiency of the reaction using a given catalyst using the TOF value, it is also necessary to specify the degree of conversion at which the given number was obtained. Author suggests that it is more understandable and accurate to give a constant rate of reaction and reaction rate instead of using the TOF values [38].

Kozuch and Martin [37] have reported that TOF value may gives kinetic information as opposed to TON which provide stoichiometric information about the catalytic process. The authors of the work [37] have claimed that “Turnover number (TON) expresses the maximum yield of products available from the catalytic center. Due to the fact that the reactivity of the investigated catalyst in selected reaction should be given by determining the rate law of the investigated process [38]. In chemical kinetics, the variables are concentrations, not activity. Concentrations of reacting reagents are required, but their values are not standard [39]. The authors [38, 39] declared also that the TOF values should be also expressed at saturation together with the concentration value. The authors also note that important information when comparing catalyst performance should be accurate information on the conditions of the reaction in which the specified reaction yield was achieved. Expressing the efficiency of the catalyst as TON or TOF, we should also provide information on how these values were obtained and provide a description of their calculation of the number of active sites, using a certain transparent and reproducible method. Summarizing the above mentioned suggestions, in order to compare the catalytic yield of various catalysts it is extremely important, that the obtained values represent intrinsic rates and selectivities. It is also important, that the obtained values of TOF and TON and selectivities be accurate, reproducible and the calculated without any restrictions on mass or heat transfer. In addition, the obtained values should apply to a wide range of conversions [37–39]. Based on the above suggestions, we decided to compare the performance of the catalysts by calculating for

these systems the reaction rate and activation energy values determined at low conversion to avoid diffusion limitation.

The results obtained for all tested catalysts showed that the system containing 20 wt% of Cu had the highest value of reaction rate and the lowest value of activation energy. This result explain the highest activity of 20%Cu/CeO<sub>2</sub>·Al<sub>2</sub>O<sub>3</sub> catalyst in the oxy-steam reforming of methanol reaction compared to the other investigated systems. In the case of the copper catalysts with lower (5%) and higher (40%) of copper loading we detected lower methanol conversion and together with higher activation energy and lower reaction rate at the investigated reaction temperature (see Table 2).

It is well known that the oxy-steam reforming of methanol reaction took place not only on the metallic Cu but also on Cu<sup>+</sup> ions species [39]. The amount of the copper species present on the catalyst surface determines the catalytic activity of the prepared copper catalysts in many various reactions especially in the case of methanol synthesis and its conversion to hydrogen. That is why the proper catalyst activation is an important process to achieve the high active copper catalysts. In this work, we activated the catalysts in a mixture of 5%H<sub>2</sub>–95%Ar prior to the catalytic activity tests. It is well known that the quantity of the metallic copper and Cu<sub>2</sub>O on the catalyst surface and their relationship is very important from the catalytic point of view. Therefore, the reduction behaviour of binary oxide carrier and monometallic copper catalysts was also investigated in this work. The temperature programmed reduction measurements were used to determine the reduction behaviour of monometallic copper supported catalysts. The TPR-H<sub>2</sub> technique is also a powerful technique which is used to study the interaction between the active phase component and binary oxide support of the prepared catalysts. To better understand the reduction properties of monometallic catalysts first we studied the reducibility of CeO<sub>2</sub>·Al<sub>2</sub>O<sub>3</sub> support. The reduction profiles of CeO<sub>2</sub>·Al<sub>2</sub>O<sub>3</sub> support and monometallic copper Cu/CeO<sub>2</sub>·Al<sub>2</sub>O<sub>3</sub> (metal loading = 5, 20, 40 and 60 wt%) catalysts are shown in Fig. 2. H<sub>2</sub>-TPR profile recorded for CeO<sub>2</sub>·Al<sub>2</sub>O<sub>3</sub> support showed the reduction effects in a wide temperature range, which are assigned with different oxide species reduction present on the surface and with the reduction of the bulk CeO<sub>2</sub>. The reduction profile recorded for the binary oxide support showed the reduction effects in the temperature range 400–600 °C, which are associated with a reduction of the surface oxygen species from the cerium (IV) oxide according to the following scheme: CeO<sub>2</sub> → CeO<sub>2-x</sub>. The high temperature effect located at about 900 °C was assigned to the reduction of bulk CeO<sub>2</sub> to Ce<sub>2</sub>O<sub>3</sub> oxide [40]. These results agree well with the reduction measurements reported by Nevanperä et al. [41]. Authors observed the same reduction stages as in our case. While, in the work [42] authors also reported about the low and the high temperature reduction stages. The low temperature reduction effect they assigned to the reduction of surface oxygen species from the cerium (IV) oxide. The high hydrogen consumption peak located at about 850 °C is associated with the reduction of bulk CeO<sub>2</sub> oxide. Then in the next part of the reducibility studies we were also investigated the reduction of monometallic copper supported catalysts. The reducibility studies were presented in Fig. 2.

TPR profile of 5% Cu/CeO<sub>2</sub>·Al<sub>2</sub>O<sub>3</sub> catalyst showed two unresolved reduction effects located in the temperature range 180–300 °C, which can be assigned to the two-steps reduction of copper(II) oxide to metallic copper via intermediate

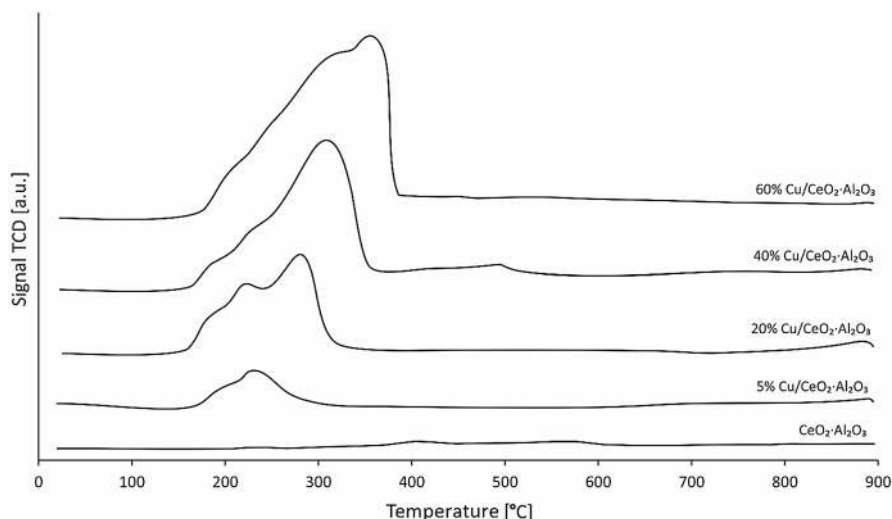


**Fig. 2** TPR profiles of  $\text{CeO}_2\cdot\text{Al}_2\text{O}_3$  support and  $\text{Cu}/\text{CeO}_2\cdot\text{Al}_2\text{O}_3$  (metal loading = 5, 20, 40 and 60 wt%) catalysts calcined in air atmosphere for 4 h at 400 °C

$\text{Cu}_2\text{O}$ . However, the temperature range of reduction profiles located on the TPR curve recorded for this system may indicate also that these reduction effects can be also associated with the reduction of small and large  $\text{CuO}$  species located on support surface. The higher temperature reduction effects are also connected with a reduction of the surface oxygen species from the cerium (IV) oxide  $\text{CeO}_2$  to superficial  $\text{CeO}_{2-x}$  species. While, the high temperature reduction peak situated at about 900 °C is assigned to the reduction of bulk  $\text{CeO}_2$  to  $\text{Ce}_2\text{O}_3$  [43]. The other authors [44] also studied the reducibility of  $\text{Cu}/\text{CeO}_2$  systems and reported about the possible reduction of support. They have suggested such action on the basis of  $\text{H}_2$  uptake by reduction of calcined  $\text{CuO}/\text{CeO}_2$  system. They conclude that much higher  $\text{H}_2$  uptake is assigned to spillover of hydrogen onto the support causing by small particles resulting in a reduction of both copper oxide and the surface of the  $\text{CeO}_2$  [45].  $\text{H}_2$ -TPR profiles recorded for other investigated copper catalysts exhibited similar reduction behaviour as for monometallic catalyst with the lowest copper content. First two unresolved reduction peaks located at low temperature range (180–380 °C) are assigned to the reduction of  $\text{CuO}$  crystallite species to metallic copper through intermediate  $\text{Cu}_2\text{O}$  species. Whereas, the high temperature reduction effects are connected with a reduction of  $\text{CeO}_2 \rightarrow \text{CeO}_{2-x}$  (400–600 °C) and  $\text{CeO}_2 \rightarrow \text{Ce}_2\text{O}_3$  (850 °C–900 °C) species and were visible for copper catalysts with higher copper loading. Furthermore, the reduction effects observed for 40%  $\text{Cu}/\text{CeO}_2\cdot\text{Al}_2\text{O}_3$  and 60%  $\text{Cu}/\text{CeO}_2\cdot\text{Al}_2\text{O}_3$  are shifted towards higher temperature range. Turco et al. [46]. studied the reducibility of copper supported catalysts and reported about two-stage reduction of the copper(II) oxide according to the following scheme  $\text{Cu}^{2+} \rightarrow \text{Cu}^+ \rightarrow \text{Cu}^0$ . However, the size and shape of these peaks indicated that this hydrogen consumption peaks may be also assigned to the reduction of two crystallites size of the copper(II) oxide [47]. Agrell et al. [48]. studied also the reduction

of various copper supported catalysts. They also reported about the reduction effect with maximum of hydrogen consumption peak at 240 °C associated with the reduction of CuO crystallites. The presences of two reduction peaks they are connected with reduction of different crystallites size of CuO.

It is well known in the literature [47] that in the OSRM process the acid centers plays an important role because of the fact that they take a part in a stabilising process of the intermediates formed during the reaction. The total acidity and the distribution of acidic centers on the catalyst surface was determined by the temperature programmed desorption of ammonia (TPD-NH<sub>3</sub>) measurements. Table 3 presents the distribution of acid centers on the catalyst surface, which was estimated based on the surface under the peaks at an appropriate temperature range. The performed TPD-NH<sub>3</sub> measurements confirmed the presence of three types of acid centers; weak, medium and strong which were detected for all investigated catalyst systems. The value of the total acidity calculated for CeO<sub>2</sub>·Al<sub>2</sub>O<sub>3</sub> support was 0.33 mmol/g. It is also worth noticing that the highest total acidity showed copper catalyst with the lowest copper loading. The results clearly show that the value of a total acidity decreases with increasing of the copper content in the examined supported catalysts. It is worth emphasizing that the catalysts with the higher content of Cu equal 20, 40 and 60 wt% in the investigated catalysts exhibited total acidity equal 0.23, 0.19 and 0.18 mmol of desorbed ammonia per gram of the catalyst, respectively. While, copper catalyst 5% Cu/CeO<sub>2</sub>·Al<sub>2</sub>O<sub>3</sub> showed additionally the highest quantity of weak and medium centers present on the catalyst surface compared to the other catalyst systems. Only carrier material exhibited higher quantity of the strong acid centres on its surface.

The phase composition studies were also performed for investigated material in this work. The X-ray diffraction technique were recorded for various monometallic copper supported catalysts Cu/CeO<sub>2</sub>·Al<sub>2</sub>O<sub>3</sub> (metal loading = 5, 20, 40 and 60 wt%) and in order to determine the possible interaction which may take place between an active phase component of the catalyst and the CeO<sub>2</sub>·Al<sub>2</sub>O<sub>3</sub> support. The XRD curves recorded for copper supported catalysts showed the occurrence of crystallographic phases such as: CuO, CeO<sub>2</sub> and  $\gamma$ -Al<sub>2</sub>O<sub>3</sub>. The detailed analysis of the recorded XRD patterns showed the occurrence of the diffraction peaks attributed to

**Table 3** The amount of NH<sub>3</sub> desorbed from the surface of Cu/CeO<sub>2</sub>·Al<sub>2</sub>O<sub>3</sub> catalysts (Cu loading = 5, 20, 40 and 60 wt%) calcined in air atmosphere at 400 °C for 4 h calculated based on the surface under the TPD-NH<sub>3</sub> profile recorded for each system

Catalysts	Total acidity (mmol/g)	Weak centers (mmol/g)	Medium centers (mmol/g)	Strong centers (mmol/g)
	180–600 °C	180–300 °C	300–450 °C	450–600 °C
CeO <sub>2</sub> ·Al <sub>2</sub> O <sub>3</sub>	0.33	0.10	0.10	0.13
5% Cu/CeO <sub>2</sub> ·Al <sub>2</sub> O <sub>3</sub>	0.54	0.19	0.25	0.10
20% Cu/CeO <sub>2</sub> ·Al <sub>2</sub> O <sub>3</sub>	0.23	0.11	0.09	0.03
40% Cu/CeO <sub>2</sub> ·Al <sub>2</sub> O <sub>3</sub>	0.19	0.09	0.08	0.02
60% Cu/CeO <sub>2</sub> ·Al <sub>2</sub> O <sub>3</sub>	0.18	0.09	0.07	0.02

the crystallographic phases assigned to  $\text{CeO}_2$  (positioned at  $2\theta$  angle:  $28.6^\circ$ ,  $33.3^\circ$ ,  $47.6^\circ$ ,  $56.5^\circ$ );  $\text{CuO}$  (positioned at  $2\theta$  angle:  $33.3^\circ$ ,  $35.6^\circ$ ,  $38.8^\circ$ ,  $48.8^\circ$ ,  $53.5^\circ$ ,  $58.4^\circ$ ,  $61.6^\circ$ ) and  $\gamma\text{-Al}_2\text{O}_3$  (positioned at  $2\theta$  angle:  $46.4^\circ$ ) (see Fig. 3) phases. The lack of diffraction peaks which could be assigned to  $\text{CuO}$  phase is explained by the limit of the XRD technique detection [44]. In the case of this system the  $\text{CuO}$  particles are highly dispersed on  $\text{CeO}_2\cdot\text{Al}_2\text{O}_3$  support and they are too small to detect by the diffractometer. This means that crystallites of  $\text{CuO}$  should be below 5 nm which are present on the catalyst surface and are not visible on diffraction pattern [12]. On the XRD diffraction curve of the catalyst system containing 20 wt% of Cu, the peaks corresponding to  $\text{CuO}$  phase are observed and their intensity increases with the increase of copper loading, which is consistent with the literature data [49, 50].

The catalytic activity and selectivity to the obtained products in the oxy-steam reforming of methanol process were also studied in this work in order to correlate their reactivity with their physicochemical properties (see Table 4 and Fig. 4). In addition, the kinetics studies were also performed for monometallic catalysts with a conversion rate of up to 10%. The activity results expressed as methanol conversion and selectivity to the all products obtained for monometallic supported catalysts showed that the highest methanol conversion at 160 and 200 °C were obtained for copper supported catalysts containing 20 wt% of Cu. The increase or decrease of the copper content in the investigative catalysts did not improve the activity of the copper based catalyst (see Fig. 4). The results of the catalytic activity showed that the selectivity to hydrogen generation is higher for the catalysts tested at 200 °C. The only difference was observed for catalyst containing the highest copper content in the investigative systems, which exhibited higher hydrogen production rate at lower temperature of the process. It is very interesting, that the activity results obtained for monometallic supported catalysts confirmed that for all catalysts any CO formation as a by-product of

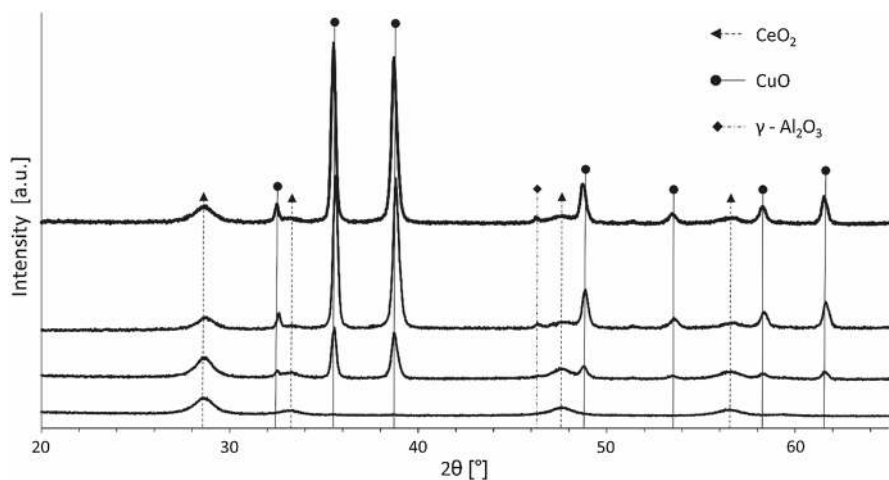


**Fig. 3** XRD patterns of  $\text{Cu/CeO}_2\cdot\text{Al}_2\text{O}_3$  (metal loading = 5, 20, 40 and 60 wt%) catalysts calcined in an air atmosphere at 400 °C for 4 h

**Table 4** Activity and selectivity results in the oxy-stream reforming of methanol over monometallic copper catalysts supported on binary oxide system

Catalyst	Temperature (°C)	CH <sub>3</sub> OH conversion (%)	H <sub>2</sub> selectivity (%)	CO selectivity (%)	CO <sub>2</sub> selectivity (%)	DME selectivity (%)
5% Cu/CeO <sub>2</sub> -Al <sub>2</sub> O <sub>3</sub>	160	47.5	57.1	0	42.9	0
	200	97.7	69.1	0	30.6	0.3
20% Cu/CeO <sub>2</sub> -Al <sub>2</sub> O <sub>3</sub>	160	60.8	23.3	0	76.7	0
	200	99.6	68.2	0	31.7	0.1
40% Cu/CeO <sub>2</sub> -Al <sub>2</sub> O <sub>3</sub>	160	11.4	51.1	0	48.9	0
	200	87.9	65.7	0	33.8	0.5
60% Cu/CeO <sub>2</sub> -Al <sub>2</sub> O <sub>3</sub>	160	0.1	75	0	25	0
	200	9.6	28.5	0	71.5	0

Reaction condition: weight of catalyst = 0.2 g, H<sub>2</sub>O/CH<sub>3</sub>OH/O<sub>2</sub> molar ratio in the feed gas = 1/1/0.4, reaction temperature = 160 and 200 °C, atmospheric pressure, GHSV = 26,700 h<sup>-1</sup>

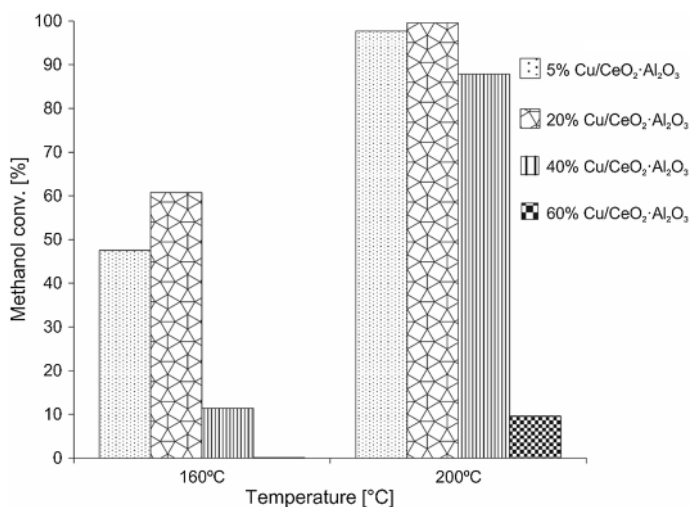


**Fig. 4** The methanol conversion in the oxy-stream reforming of methanol over Cu/CeO<sub>2</sub>-Al<sub>2</sub>O<sub>3</sub> catalysts (metal loading = 5, 20, 40 and 60 wt%). Reaction condition: weight of catalyst = 0.1 g, H<sub>2</sub>O/CH<sub>3</sub>OH/O<sub>2</sub> molar ratio in the reaction mixture = 1/1/0.4, temperature of the reaction 160 and 200 °C. The catalytic tests were performed under atmospheric pressure (GHSV = 26,700 h<sup>-1</sup>)

the process was not observed. This tendency is very important from the application point of view of the use of these types of catalysts in fuel cell technology. In addition, we should remember that the lack of the CO in the effluent gas can be related also with the limitation of the TCD detector [8]. The reactivity results showed that at 200 °C the catalysts containing 5 and 20 wt% of Cu were comparable high active and showed above 95% of methanol conversion and high selectivity towards hydrogen generation above 68%. While, in the

case of the monometallic copper catalysts with higher copper content (40 and 60% wt of Cu) the catalytic activity performed in OSRM showed that methanol conversion decreases at both temperatures. This decrease of the methanol conversion is significant especially in the case of the catalyst with the highest copper content (60 wt% of Cu) in the system, reaching the value of about 10% at 200 °C. The results of the activity measurements gave clear evidence that the only by-product in this process was dimethyl ether which was formed in small quantities. Analogical catalytic measurements in OSRM process over copper catalysts supported on CeO<sub>2</sub> were investigated by Udani and co-workers [44]. They reported that methanol conversion and CO selectivity in the investigated process increased parallel with growth of the metal content in the studied system up to 70 atom %. Above this value methanol conversion decrease and the light-off temperature for all catalysts was 180 °C. In our work the highest methanol conversion values were obtained for copper catalysts supported on binary oxide at 200 °C. The same light-off temperature for copper catalysts was reported by Perez-Hernández et al. [51].

## Conclusions

In this work monometallic catalysts supported on binary oxide CeO<sub>2</sub>–Al<sub>2</sub>O<sub>3</sub> were prepared by impregnation method and tested in oxy-steam reforming of methanol process. The catalytic activity tests performed in OSRM reaction showed that the most active system was 20%/CeO<sub>2</sub>–Al<sub>2</sub>O<sub>3</sub> which exhibited 99.6% of methanol conversion and 68.2% selectivity to hydrogen formation. It is worth to emphasize that any of the studied catalysts did not exhibited the CO formation during OSRM process. This result also confirms the potential of usage of the copper catalysts system supported on binary oxide in Fuel cell technology to generate electricity. In addition, it is also important that the most active 20%/CeO<sub>2</sub>–Al<sub>2</sub>O<sub>3</sub> system exhibited also the lowest value of energy activation and the highest reaction rate in OSRM process compared to the rest of the catalysts. It should be also noticed that at 200 °C the catalysts containing 5 and 20 wt% of Cu exhibited comparable activity above 95% of methanol conversion and high selectivity towards hydrogen generation above 68%. In addition, 20%/CeO<sub>2</sub>–Al<sub>2</sub>O<sub>3</sub> system showed also high specific surface area and total acidity compared to the catalysts with high copper loading (40 and 60 wt% of Cu).

**Acknowledgements** The project was funded by the National Science Centre (Opus 15 Programme - Grant No. 2018/29/B/ST8/01317). Magdalena Mosinska thanks the Lodz University of Technology for a scholarship (Własny Fundusz Stypendialny PE programme, Nr RNN/WFS/25/2018).

## Compliance with ethical standards

**Conflict of interest** The authors declare that there is no conflict of interest regarding the publication of this paper.

**Open Access** This article is distributed under the terms of the Creative Commons Attribution 4.0 International License (<http://creativecommons.org/licenses/by/4.0/>), which permits unrestricted use, distribution, and reproduction in any medium, provided you give appropriate credit to the original author(s) and the source, provide a link to the Creative Commons license, and indicate if changes were made.

## References

1. Mierczynski P, Mierczynska A, Ciesielski R, Maniukiewicz W, Rogowski J, Maniecki Tomasz P, Dubkov S, Sysa A, Gromov D, Szyrkowska MI, Vasilev K (2018) Modern Ni and Pd–Ni catalysts supported on Sn–Al binary oxide for oxy-steam reforming of methanol. *Energy Technol* 6:1687–1699
2. Patel S, Pant KK (2006) Influence of preparation method on performance of Cu(Zn)(Zr)-alumina catalysts for the hydrogen production via steam reforming of methanol. *J Porous Mater* 13:373–378
3. Patel S, Pant KK (2006) Production of hydrogen with low carbon monoxide formation via catalytic steam reforming of methanol. *J Fuel Cell Sci Technol* 3:369–374
4. Sahoo DR, Vajpai S, Patel S, Pant KK (2007) Kinetic modeling of steam reforming of ethanol for the production of hydrogen over Co/Al<sub>2</sub>O<sub>3</sub> catalyst. *Chem Eng J* 125:139–147
5. Semelsberger TA, Ott KC, Borup RL, Greene HL (2006) Generating hydrogen-rich fuel-cell feeds from dimethyl ether (DME) using Cu/Zn supported on various solid-acid substrates. *Appl Catal A* 309:210–223
6. Patel S, Pant KK (2006) Activity and stability enhancement of copper–alumina catalysts using cerium and zinc promoters for the selective production of hydrogen via steam reforming of methanol. *J Power Sour* 159:139–143
7. Patel S, Pant KK (2007) Hydrogen production by oxidative steam reforming of methanol using ceria promoted copper–alumina catalysts. *Fuel Process Technol* 88:825–832
8. Mierczynski P, Vasilev K, Mierczynska A, Maniukiewicz W, Ciesielski R, Rogowski J, Szyrkowska IM, Trifonov AY, Dubkov SV, Gromov DG, Maniecki TP (2016) The effect of gold on modern bimetallic Au–Cu/MWCNT catalysts for the oxy-steam reforming of methanol. *Catal Sci Technol* 6:4168–4183
9. Selva Roselin L, Chiu HW (2018) Production of hydrogen by oxidative steam reforming of methanol over Cu/SiO<sub>2</sub> catalysts. *J Saudi Chem Soc* 22:692–704
10. Mierczynski P, Mosinska M, Zakrzewski M, Dawid B, Ciesielski R, Maniukiewicz W, Maniecki T (2017) Influence of the Zn–Al binary oxide composition on the physicochemical and catalytic properties of Ni catalysts in the oxy-steam reforming of methanol. *React Kinet Mech Cat* 121:453–472
11. Mierczynski P (2016) Comparative studies of bimetallic Ru–Cu, Rh–Cu, Ag–Cu, Ir–Cu catalysts supported on ZnO–Al<sub>2</sub>O<sub>3</sub>, ZrO<sub>2</sub>–Al<sub>2</sub>O<sub>3</sub> systems. *Catal Lett* 146:1825–1837
12. Mierczynski P, Vasilev K, Mierczynska A, Maniukiewicz W, Szyrkowska MI, Maniecki TP (2016) Bimetallic Au–Cu, Au–Ni catalysts supported on MWCNTs for oxy-steam reforming of methanol. *Appl Catal B* 185:281–294
13. Velu S, Suzuki K, Kapoor MP, Ohashi F, Osaki T (2001) Selective production of hydrogen for fuel cells via oxidative steam reforming of methanol over CuZnAl(Zr)-oxide catalysts. *Appl Catal A* 213:47–63
14. Trovarelli A (1996) Catalytic Properties of Ceria and CeO<sub>2</sub>-containing materials. *Catal Rev* 38:439–520
15. Men Y, Gnaser H, Ziegler C, Zapf R, Hessel V, Kolb G (2005) Characterization of Cu/CeO<sub>2</sub>/γ-Al<sub>2</sub>O<sub>3</sub> thin film catalysts by thermal desorption spectroscopy. *Catal Lett* 105:35–40
16. Men Y, Gnaser H, Zapf R, Hessel V, Ziegler C (2004) Parallel screening of Cu/CeO<sub>2</sub>/γ-Al<sub>2</sub>O<sub>3</sub> catalysts for steam reforming of methanol in a 10-channel micro-structured reactor. *Catal Commun* 5:671–675
17. Liu Y, Hayakawa T, Suzuki K, Hamakawa S, Tsunoda T, Ishii T, Kumagai M (2002) Highly active copper/ceria catalysts for steam reforming of methanol. *Appl Catal A* 223:137–145
18. Chang CC, Chang CT, Chiang SJ, Liaw BJ, Chen YZ (2010) Oxidative steam reforming of methanol over CuO/ZnO/CeO<sub>2</sub>/ZrO<sub>2</sub>/Al<sub>2</sub>O<sub>3</sub> catalysts. *Int J Hydrog Energy* 35:7675–7683
19. Tonelli F, Gorriz O, Tarditi A, Cornaglia L, Arrúa L, Cristina Abello M (2015) Activity and stability of a CuO/CeO<sub>2</sub> catalyst for methanol steam reforming. *Int J Hydrog Energy* 40:13379–13387



20. Oguchi H, Nishiguchi T, Matsumoto T, Kanai H, Utani K, Matsumura Y, Imamura S (2005) Steam reforming of methanol over Cu/CeO<sub>2</sub>/ZrO<sub>2</sub> catalysts. *Appl Catal A* 281:69–73
21. Jones SD, Hagelin-Weaver HE (2009) Steam reforming of methanol over CeO<sub>2</sub>- and ZrO<sub>2</sub>-promoted Cu–ZnO catalysts supported on nanoparticle Al<sub>2</sub>O<sub>3</sub>. *Appl Catal B* 90:195–204
22. Barrios CE, Bosco MV, Baltanás MA, Bonivardi AL (2015) Hydrogen production by methanol steam reforming: catalytic performance of supported-Pd on zinc–cerium oxides nanocomposites. *Appl Catal B* 179:262–275
23. Dey S, Mohan D, Dhal GC, Prasad R (2018) Copper based mixed oxide catalysts (CuMnCe, CuMnCo and CuCeZr) for the oxidation of CO at low temperature. *Mater Discov* 10:1–14
24. Lykaki M, Pachaturidou E, Carabineiro SAC, Iliopoulou E, Andriopoulou C, Kallithrakas-Kontos N, Boghosian S, Konsolakis M (2018) Ceria nanoparticles shape effects on the structural defects and surface chemistry: implications in CO oxidation by Cu/CeO– catalysts. *Appl Catal B* 230:18–28
25. Jing G, Zhang X, Zhang A, Li M, Zeng S, Xu C, Su H (2018) CeO<sub>2</sub>–CuO/Cu<sub>2</sub>O/Cu monolithic catalysts with three-kind morphologies Cu<sub>2</sub>O layers for preferential CO oxidation. *Appl Surf Sci* 434:445–451
26. Barrio L, Estrella M, Zhou G, Wen W, Hanson JC, Hungria AB, Hornés A, Fernández-García M, Martínez-Arias A, Rodríguez JA (2010) Unraveling the active site in copper–Ceria Systems for the water–gas shift reaction. In situ characterization of an inverse powder CeO<sub>2</sub>–x/CuO–Cu catalyst. *J Phys Chem C* 114:3580–3587
27. Rodríguez JA, Grinter DC, Liu Z, Palomino RM, Senanayake SD (2017) Ceria-based model catalysts: fundamental studies on the importance of the metal–ceria interface in CO oxidation, the water–gas shift, CO<sub>2</sub> hydrogenation, and methane and alcohol reforming. *Chem Soc Rev* 46:1824–1841
28. Poggio-Fraccari E, Giunta P, Baronetti G, Mariño F (2017) Cu and/or Ni catalysts over CePr oxide for the water gas shift reaction: an experimental study, kinetic fitting and reactor simulation. *React Kinet Mech Cat* 121:607–628
29. Mierczynski P, Maniecki T, Maniukiewicz W, Jozwiak W (2011) Cu/Cr<sub>2</sub>O<sub>3</sub>·3Al<sub>2</sub>O<sub>3</sub> and Au–Cu/Cr<sub>2</sub>O<sub>3</sub>·3Al<sub>2</sub>O<sub>3</sub> catalysts for methanol synthesis and water gas shift reactions. *React Kinet Mech Cat* 104:139–148
30. Mierczynski P, Maniukiewicz W, Maniecki T (2013) Comparative studies of Pd, Ru, Ni, Cu/ZnAl<sub>2</sub>O<sub>4</sub> catalysts for the water gas shift reaction. *Open Chem* 11:912–919
31. Graciani J, Mudiyansele K, Xu F, Baber AE, Evans J, Senanayake SD, Stacchiola DJ, Liu P, Hrbek J, Sanz JF, Rodríguez JA (2014) Highly active copper–ceria and copper–ceria–titania catalysts for methanol synthesis from CO<sub>2</sub>. *Science* 345:546
32. Ouyang B, Tan W, Liu B (2017) Morphology effect of nanostructure ceria on the Cu/CeO<sub>2</sub> catalysts for synthesis of methanol from CO<sub>2</sub> hydrogenation. *Catal Commun* 95:36–39
33. Mierczynski P, Ciesielski R, Kedziora A, Shtyka O, Maniecki TP (2016) Methanol synthesis using copper catalysts supported on CeO<sub>2</sub>–Al<sub>2</sub>O<sub>3</sub> mixed oxide. *Fibre Chem* 48:271–275
34. Jackson MA, White MG, Haasch RT, Peterson SC, Blackburn JA (2018) Hydrogenation of furfural at the dynamic Cu surface of CuO/CeO<sub>2</sub>/Al<sub>2</sub>O<sub>3</sub> in a vapor phase packed bed reactor. *Mol Catal* 445:124–132
35. Jiménez-Gómez CP, Cecilia JA, Márquez-Rodríguez I, Moreno-Tost R, Santamaría-González J, Mérida-Robles J, Maireles-Torres P (2017) Gas-phase hydrogenation of furfural over Cu/CeO<sub>2</sub> catalysts. *Catal Today* 279:327–338
36. Bligaard T, Bullock RM, Campbell CT, Chen JG, Gates BC, Gorte RJ, Jones CW, Jones WD, Kitchin JR, Scott SL (2016) Toward benchmarking in catalysis science: best practices, challenges, and opportunities. *ACS Catal* 6:2590–2602
37. Kozuch S, Martin JML (2012) “Turning over” definitions in catalytic cycles. *ACS Catal* 2:2787–2794
38. Lente G (2013) Comment on “‘turning over’ definitions in catalytic cycles”. *ACS Catal* 3:381–382
39. Mierczynski P, Vasilev K, Mierczynska A, Maniukiewicz W, Maniecki T (2013) The Effect of ZnAl<sub>2</sub>O<sub>4</sub> on the performance of Cu/ZnxAlyOx + 1.5y supported catalysts in steam reforming of methanol. *Top Catal* 56:1015–1025
40. Rynkowski JM, Paryczak T, Lewicki A, Szykowska MI, Maniecki TP, Jozwiak WK (2000) Characterization of Ru/CeO<sub>2</sub>–Al<sub>2</sub>O<sub>3</sub> catalysts and their performance in CO<sub>2</sub> methanation. *React Kinet Catal Lett* 71:55–64
41. Nevanperä TK, Ojala S, Bion N, Epron F, Keiski RL (2016) Catalytic oxidation of dimethyl disulfide (CH<sub>3</sub>SSCH<sub>3</sub>) over monometallic Au, Pt and Cu catalysts supported on γ-Al<sub>2</sub>O<sub>3</sub>, CeO<sub>2</sub> and CeO<sub>2</sub>–Al<sub>2</sub>O<sub>3</sub>. *Appl Catal B* 182:611–625

42. Andreeva D, Ivanov I, Ilieva L, Sobczak JW, Avdeev G, Tabakova T (2007) Nanosized gold catalysts supported on ceria and ceria-alumina for WGS reaction: influence of the preparation method. *Appl Catal A* 333:153–160
43. Si R, Raitano J, Yi N, Zhang L, Chan SW, Flytzani-Stephanopoulos M (2012) Structure sensitivity of the low-temperature water-gas shift reaction on Cu–CeO<sub>2</sub> catalysts. *Catal Today* 180:68–80
44. Udani PPC, Gunawardana PVDS, Lee HC, Kim DH (2009) Steam reforming and oxidative steam reforming of methanol over CuO–CeO<sub>2</sub> catalysts. *Int J Hydrog Energy* 45:7648–7655
45. Pérez-Hernández R, Aguilar F, Gómez-Cortés A, Díaz G (2005) NO reduction with CH<sub>4</sub> or CO on Pt/ZrO<sub>2</sub>–CeO<sub>2</sub> catalysts. *Catal Today* 107–108:175–180
46. Turco M, Bagnasco G, Costantino U, Marmottini F, Montanari T, Ramis G, Busca G (2004) Production of hydrogen from oxidative steam reforming of methanol: I. Preparation and characterization of Cu/ZnO/Al<sub>2</sub>O<sub>3</sub> catalysts from a hydrotalcite-like LDH precursor. *J Catal* 228:43–55
47. Turco M, Bagnasco G, Cammarano C, Senese P, Costantino U, Sisani M (2007) Cu/ZnO/Al<sub>2</sub>O<sub>3</sub> catalysts for oxidative steam reforming of methanol: the role of Cu and the dispersing oxide matrix. *Appl Catal B* 77:46–57
48. Agrell J, Birgersson H, Boutonnet M, Melián-Cabrera I, Navarro RM, Fierro JLG (2003) Production of hydrogen from methanol over Cu/ZnO catalysts promoted by ZrO<sub>2</sub> and Al<sub>2</sub>O<sub>3</sub>. *J Catal* 219:389–403
49. Gunawardana PVDS, Lee HC, Kim DH (2009) Performance of copper–ceria catalysts for water gas shift reaction in medium temperature range. *Int J Hydrog Energy* 34:1336–1341
50. Zhu P, Li J, Zuo S, Zhou R (2008) Preferential oxidation properties of CO in excess hydrogen over CuO–CeO<sub>2</sub> catalyst prepared by hydrothermal method. *Appl Surf Sci* 255:2903–2909
51. Pérez-Hernández R, Gutiérrez-Martínez A, Gutiérrez-Wing CE (2007) Effect of Cu loading on CeO<sub>2</sub> for hydrogen production by oxidative steam reforming of methanol. *Int J Hydr Energy* 32:2888–2894

**Publisher's Note** Springer Nature remains neutral with regard to jurisdictional claims in published maps and institutional affiliations.